



1 **A chironomid-based record of temperature variability during the**
2 **past 4000 years in northern China and its possible societal**
3 **implications**

4 Haipeng Wang ¹, Jianhui Chen ^{2*}, Shengda Zhang ³, David D. Zhang ³, Zongli Wang ², Qinghai Xu
5 ⁴, and Fahu Chen ²

6

7 ¹*State Key Laboratory of Cryospheric Science, Northwest Institute of Eco-Environment and*
8 *Resources, Chinese Academy of Sciences, Lanzhou 730000, China*

9 ²*MOE Key Laboratory of Western China's Environmental Systems, College of Earth*
10 *Environmental Sciences, Lanzhou University, Lanzhou 73000, China*

11 ³*Department of Geography, The University of Hong Kong, Hong Kong, China*

12 ⁴*Institute of Nihewan Archaeology Research, Hebei Normal University, Shijiazhuang 050024,*
13 *China*

14 * *Author for correspondence (email: jhchen@lzu.edu.cn)*

15

16 **Abstract:** Long-term, high-resolution temperature records which combine an unambiguous
17 proxy and precise dating are rare in China. In addition, the societal implications of past
18 temperature change on regional scale have not been sufficiently assessed. Here, based on the
19 modern relationship between chironomids and temperature, we use fossil chironomid
20 assemblages in a precisely-dated sediment core from Gonghai Lake to explore temperature



21 variability during the past 4000 years in northern China. Subsequently, we address the
22 possible regional societal implications of temperature change through a statistical analysis of
23 the occurrence of wars. Our results show that: (1) the mean annual temperature (TANN) was
24 relatively high from 4000-2700 cal yr BP, decreased gradually from 2700-1270 cal yr BP, and
25 then fluctuated drastically during the last 1270 years. (2) A cold climatic event in the Era of
26 Disunity, the Sui-Tang Warm Period (STWP), the Medieval Warm Period (MWP) and the
27 Little Ice Age (LIA) can all be recognized in the paleotemperature record, as well as in many
28 other temperature reconstructions in China. This suggests that our chironomid-inferred
29 temperature record for the Gonghai Lake region is representative. (3) Local wars in Shanxi
30 Province, documented in the historical literature during the past 2700 years, are statistically
31 significantly correlated with changes in temperature, and the relationship is a good example
32 of the potential societal implications of temperature change on a regional scale.

33 **Keywords:** chironomids, temperature change, northern China, late-Holocene, societal
34 implications

35

36 **1 Introduction**

37 Climate change presents new and significant challenges for human society, including the need
38 to understand and respond to the possible dangers (Stocker et al., 2013). Since the past is the
39 key to the present and the future, the study of past temperature changes is becoming
40 increasingly important for improving our ability to predict the long-term trends of regional
41 and global climate change, and to explore the relationship between climate change and human
42 society.



43 East Asia, a densely populated region, has attracted much research attention focused on
44 documenting the frequency and amplitude of past climate changes. While the Holocene
45 variability of the precipitation associated with the East Asian summer monsoon (EASM) has
46 been discussed in detail (e.g., Dykoski et al., 2005; Chen et al., 2015; Liu et al., 2015; Chen et
47 al., 2016; Liu et al., 2017), studies of temperature change on different temporal and spatial
48 scales may provide deeper insights to past climate fluctuations and facilitate the prediction of
49 future climate change. During the past few decades, various studies have reconstructed
50 temperature change on different time-scales in northern China, using for example pollen (e.g.,
51 Xu et al., 2010; Wen et al., 2010), GDGTs (e.g., Gao et al., 2012; Jia et al., 2013; Peterse et al.,
52 2014), stalagmites (Tan et al., 2003), and historical archives (Ge et al., 2003). However, many
53 of these temperature records have significant limitations: for example, pollen assemblages are
54 regarded as a precipitation indicator in many records in northern China (e.g., Chen et al., 2015;
55 Zhao et al., 2010), the resolution of GDGTs records is too low (although their environmental
56 significance is relatively unambiguous), and the timescales of the stalagmite records from
57 Shihua Cave, and of historical documents from East China, are too short, even if they are
58 accurately dated. All of these factors impede our understanding of paleotemperature
59 variability during the Holocene, and in addition there is a mismatch between model
60 simulations of a cooler-than-baseline annual temperature series during the late Holocene
61 compared to the present climate (Jiang et al., 2012) and multi-proxy reconstructions of the
62 mid-Holocene megathermal in China (e.g., Shi et al., 1993; Wang et al., 2001; Peterse *et al.*,
63 2011; Huang et al., 2013). Thus, a long-term, high-resolution paleotemperature reconstruction,
64 using an unequivocal proxy with a robust chronology, is needed.

65 Chironomids, benthic invertebrates, are recognized as a reliable paleotemperature proxy
66 because of their stenotypic and environmentally-sensitive characteristics (Walker et al., 1991;
67 Levesque et al., 1997; Brooks et al., 2007; Brooks et al., 2012a). Many modern chironomid



68 training sets have been established and used for paleoenvironment reconstruction (especially
69 paleotemperature) worldwide (e.g., Walker and Cwynar, 2006; Rees et al., 2008; Eggermont
70 et al., 2010; Heiri et al., 2011; Nazarova et al., 2011; Massafiero and Larocque-Tobler, 2013).
71 The paleoenvironmental application of chironomid analysis is relatively recent in China, and
72 studies have concentrated mainly on lake ecology, including analysis of total phosphorus in
73 the middle and lower reaches of the Yangtze River (Zhang et al., 2006), salinity on the
74 Tibetan Plateau (Zhang et al., 2007; Chen et al., 2009), lake water-depth in the arid region of
75 northwest China (Chen et al., 2014), and precipitation near the EASM boundary (Wang et al.,
76 2016). Currently, there is only one chironomid-based temperature record, which was obtained
77 from the southeastern Tibetan Plateau (Zhang et al., 2017a and 2017b).

78 Here, we present the results of a study of chironomid assemblages in a sediment core from
79 Gonghai Lake in northern China, with the aim of reconstructing regional temperature
80 variability during the past 4000 years in northern China. Gonghai Lake, a freshwater
81 closed-basin lake in Shanxi Province (Fig. 1a), was previously shown to be suitable for
82 chironomid studies (Wang et al., 2016). A modern calibration data set consisting of 44 fresh
83 water bodies in the area has been developed by Wang *et al.* (2016). Although this data set
84 suggested that chironomid assemblages in the area responded significantly to fluctuations in
85 water depth since the last deglaciation (Wang et al., 2016), the typical stenothermal species
86 were still sensitive to paleotemperature variability at various time scales. In addition, as well
87 as having significant regional environmental effects, past climate change may also have
88 triggered human societal crises (Zhang et al., 2015). Numerous studies have demonstrated a
89 strong temporal relationship between societal crises and climate change, and a recent study
90 indicated that climate change (especially temperature) was the ultimate cause of a large-scale
91 human crisis in preindustrial Europe and the Northern Hemisphere (Zhang et al., 2011).
92 However, most of the previous research has focused on the human societal response to



93 climate change on a large spatial scale and the response on a regional scale has rarely been
94 considered. The aim of the present study is to use a chironomid-based temperature record
95 from Gonghai Lake spanning the past 4000 years to test the hypothesis that human societal
96 crises were an indirect consequence of temperature fluctuations at the regional scale. Thus, in
97 the present study, we (i) identify typical warm- and cold-preference chironomid taxa as
98 temperature indicators, based on the modern calibration set and previous ecological
99 understanding from the literature; (ii) estimate past temperature variability by analyzing the
100 percentage changes in warm- and cold-preference taxa, and validate its reliability; and (iii)
101 compare the temperature record with the documented occurrence of wars in Shanxi Province.

102 **2 Regional setting**

103 Gonghai Lake (38°54' N, 112°14' E; 1,860 m.a.s.l), an alpine freshwater lake, is situated on
104 the northeastern margin of the Chinese Loess Plateau (Fig. 1a). The lake is oval-shaped and
105 has a surface area of $\sim 0.36 \text{ km}^2$, a maximum water depth of around 10 m, and a flat
106 bottom-topography (Fig. 1b). The lake may have been formed by tectonic activity at around
107 $\sim 16 \text{ ka BP}$ (Wang et al., 2014). On average, 77 % of the 445 mm of modern annual
108 precipitation occurs from June to September and is the major water source since the lake is
109 hydrologically closed. Modern mean monthly temperature in the region ranges between
110 $-14 \text{ }^\circ\text{C}$ and $+23 \text{ }^\circ\text{C}$. In 2009, a 9.42-m-long sediment core (GH09B) was taken at a water
111 depth of 8.96 m (Fig. 1b) using a Uwitec Piston Corer. The core was sliced at 1-cm intervals,
112 freeze-dried and stored at $4 \text{ }^\circ\text{C}$ in the laboratory. In the present study, 109 samples from the
113 upper 541 cm were processed for chironomid analysis. Several adjacent samples which
114 produced fewer than 30 head capsules were amalgamated. A total of 63 samples were
115 included and used for temperature analysis, of which 44 samples contained more than 40 head
116 capsules and 19 samples contained 30-40 head capsules, representing time intervals varying



117 between 50 and 100 years and spanning the past ca. 4000 years.

118 The modern calibration set from around Gonghai Lake obtained by Wang *et al.* (2016) was
 119 re-analyzed in this study to extract the temperature signals contained in the chironomid data.
 120 The data set comprises 44 water bodies in northern China (Fig. 3a), samples from only 30 of
 121 which contained sufficient chironomid head capsules for analysis.

122

123

124

Figure 1

125

126

127 **3 Methods**

128 **3.1 Chironomid samples**

129 For each sample, chironomid remains were extracted from 1-5 g of freeze-dried sediment.
 130 The preparation procedure followed the standard techniques described in Brooks *et al.* (2007).
 131 The sediments were deflocculated in warm 10 % KOH for about 15 minutes, and then sieved
 132 with 212 μm and 90 μm mesh sieves. Head capsules were hand-picked from the sieve
 133 residues under a stereomicroscope at $\times 20$ -40 magnification, and mounted on slides, ventral
 134 side up, in Hydromatrix beneath a 6-mm coverslip. Chironomid head capsules were identified
 135 to the highest possible taxonomic resolution under a compound microscope at $\times 100$ -400
 136 magnification with reference to Wiederholm (1983), Rieradevall and Brooks (2001), Brooks
 137 *et al.* (2007), Walker (2007), and the chironomid collections housed at the Natural History



138 Museum, London.

139 3.2 Environmental variables

140 In the modern calibration set, mean annual temperature (TANN), mean summer temperature
141 (summer Tem), and the mean temperatures for June (June Tem), July (July Tem) and August
142 (August Tem) were interpolated from meteorological data from 2001-2011 (Zhao et al.,
143 unpublished data). Given that most chironomid taxa respond significantly to summer or July
144 temperatures (Brooks and Birks, 2001; Self et al., 2011; Samartin et al., 2017) and barely
145 survive in winter, the mean temperature of the winter months was excluded from the selected
146 environment variables. For the Gonghai Lake sediments, the organic matter content of each
147 sample, some of which was published in Wang *et al.* (2016), was estimated using standard
148 loss-on-ignition procedures (LOI) (Heiri et al., 2001).

149 3.3 Historical documentary evidence

150 A large amount of detailed documentary evidence is available for China. This material
151 documents a wide range of human activities and it provides a valuable reference for the
152 present study. Information pertaining to wars was obtained from the *Tabulation of Wars in*
153 *Ancient China*, an appendix of the *Military History of China*, which was summarized by the
154 Editorial Committee of Chinese Military History (1985); it has been widely utilized in
155 previous research (Zhang et al., 2005, 2015). Only the ancient wars which occurred within the
156 current territory of Shanxi Province were counted in the present study. In addition,
157 fluctuations in population size are a major component of human societal evolution and
158 therefore population information was also collated and used to characterize social change.
159 Data documenting fluctuations in the population size of Shanxi Province were obtained from
160 Lu and Teng (2006).



161 3.4 Numerical analysis

162 Only taxa which were present in at least two samples with an abundance of >2 % were
 163 selected for analysis. A chironomid percentage diagram was plotted using Tilia 2.0.2 (Grimm,
 164 2004). Zonation of the chironomid assemblages was accomplished using stratigraphically-
 165 constrained cluster analysis (CONISS) in Tilia 2.0.2 (Grimm, 2004). Both redundancy
 166 analysis (RDA) and detrended correspondence analysis (DCA) were performed using R 3.2.1
 167 (R Core Team, 2014) to explore the relationship between modern chironomid taxa and
 168 temperature variables, and to analyze the distribution characteristics of fossil assemblages,
 169 respectively. In addition, Pearson correlation and Granger causality analysis were performed
 170 to explore the relationship between climate change and the occurrence of wars.

171

172 4 Chronology

173 The age model for core GH09B is based on 10 accelerator mass spectrometry (AMS) ^{14}C
 174 dates of terrestrial plant macrofossils which were calibrated to calendar years using Oxcal 4.1
 175 with the IntCal09 (Reimer et al., 2009) (Fig. 2). All the dates were published in Chen et al.,
 176 2015.

177

178

179

180

Figure 2



181

182 **5 Results**

183 5.1 Modern chironomid assemblages

184 Air temperature is widely assumed to play the dominant role in controlling the abundance and
 185 composition of chironomid taxa in freshwater (e.g., Walker, 2001; Brooks, 2003; Walker and
 186 Cwynar, 2006). RDA of the chironomid taxa and temperature variables shows that TANN
 187 tends to be more significant in influencing the chironomid assemblages than the mean
 188 temperatures of summer, June, July and August (Fig. 3b). This result also passed the Monte
 189 Carlo permutation test ($p=0.001$) even though the explanatory ability is relatively low (Fig.
 190 3b). The taxa were plotted in Fig. 3c according to the taxon scores in the RDA of chironomid
 191 assemblages and TANN. Taxa on the left side of the plot currently prefer a warmer
 192 environment in the Gonghai Lake region because they are distributed close to the positive
 193 axis of TANN in Fig. 3b; conversely, those taxa on the right side of the plot prefer a colder
 194 environment.

195 Only typical species were selected and identified as temperature indicators. The following
 196 criteria were used to select temperature-sensitive species: (1) Those located at the ends of Fig.
 197 3c, and (2) those species previously reported as warm or cold stenotherms. On the left side of
 198 the diagram, *Polypedilum nubifer*-type, *Dicrotendipes nervosus*-type and *Tanytarsus*
 199 *mendax*-type were defined as thermophilous taxa because they have been previously reported
 200 as warm stenotherms (Watson et al., 2010; Brooks and Heiri, 2013). *Procladius choreus*-type
 201 and *Microchironomus* were eliminated because their high scores on the positive axis may be
 202 because in the Gonghai Lake region they are indicators of deep water (Wang et al., 2016). On
 203 the right side of the diagram, *Chironomus gonghai*-type, *Hydrobaenus conformis*-type,



204 *Psectrocladius sordidellus*-type, and Chironomini 1st instar (probably *Sergentia coracina*-type)
 205 were defined as cold-water taxa given that *Chironomus gonghai*-type was located at the end
 206 of the diagram and it tends to live in cold environments (see Fig. 5 in Wang et al., 2016).
 207 *Hydrobaenus conformis*-type, *Psectrocladius sordidellus*-type, and Chironomini 1st instar
 208 (probably *Sergentia coracina*-type) are regarded as cold stenotherms (Cranston et al., 1983;
 209 Brodin, 1986; Brooks and Heiri, 2013).

210

211

212

Figure 3

213

214

215 5.2 Chironomid assemblages in Gonghai Lake

216 44 major taxa within 25 genera and 4 subfamilies (Tanypodinae, Chironomini, Tanytarsini
 217 and Orthocladiinae) were identified, and 3 chironomid assemblage zones were recognized
 218 (Fig. 4). 95.7 % of the chironomid head capsules were identified to genus or species
 219 morphotype. Due to poor preservation, the remaining 4.3 % were only identified to subfamily
 220 level; this was especially applicable to the head capsules of the tribe Tanypodinae because the
 221 key identification segments of fragmented subfossils were often covered by other material.
 222 The concentration of chironomid head capsules appeared to follow variations in the organic
 223 matter content of the samples. The concentration was high before 1500 cal yr BP and then
 224 decreased to very low values until the present (Fig. 4). The chironomid assemblage zones are
 225 described below.

226 *Zone 1* (ca. 4000-2700 cal yr BP). This zone is dominated by *Cladotanytarsus mancus*-type,
 227 *Procladius* and *Stictochironomus*. Many *Tanytarsini* taxa, including *Tanytarsus* ‘no spur’,



228 *Tanytarsus mendax*-type, *Tanytarsus lugens*-type and *Tanytarsus glabrescens*-type, are present
229 at a low abundance.

230 *Zone 2 (ca. 2700-1270 cal yr BP)*. This zone is characterized by the rapid decrease in the
231 abundance of *Cladotanytarsus mancus*-type and by the sudden appearance of *Parakiefferiella*
232 *bathophila*-type. In addition, there is an increasing representation of *Paratanytarsus*,
233 *Hydrobaenus conformis*-type and *Psectrocladius sordidellus*-type.

234 *Zone 3 (ca. 1270-present)*. This zone is characterized by a significant increase in
235 *Cladotanytarsus mancus*-type and a decrease in *Parakiefferiella bathophila*-type.
236 *Hydrobaenus conformis*-type remains at a relatively high level throughout the zone. There are
237 large fluctuations in the representation of most of the taxa and therefore the zone is divided
238 into the following subzones.

239 *Subzone 3a (ca. 1270-1040 cal yr BP)*. This subzone is characterised by an abrupt increase
240 of *Cladotanytarsus mancus*-type and decrease of *Parakiefferiella bathophila*-type.

241 *Subzone 3b (ca. 1040-970 cal yr BP)*. This subzone, which only consists of two samples, is
242 dominated by *Prosilocerus jacuticus*-type, *Chironomus gonghai*-type, *Chironomini larvula*
243 (probably *Sergentia coracina*-type) and *Procladius*.

244 *Subzone 3c (ca. 970-570 cal yr BP)*. Although they are very poorly represented in the
245 previous subzone, *Cladotanytarsus mancus*-type, *Parakiefferiella bathophila*-type and
246 *Hydrobaenus conformis*-type became dominant in this subzone.

247 *Subzone 3d (ca. 570-270 cal yr BP)*. In this subzone, *Psectrocladius sordidellus*-type
248 increases abruptly and reaches its maximum abundance, and *Hydrobaenus conformis*-type is
249 highly abundant throughout.



250 Subzone 3e (ca. 270 cal yr BP-present). The dominant taxon in this subzone is
 251 *Paratanytarsus penicillatus*-type. Both *Cladotanytarsus mancus*-type and *Glyptotendipes*
 252 *severini*-type increase slightly, whereas *Hydrobaenus conformis*-type and *Psectrocladius*
 253 *sordidellus*-type decrease significantly.

254

255

256

Figure 4

257

258

259 5.3 Changes in the abundance of temperature indicator species

260 Based on the definition of warm- and cold-preference taxa given above, their totals were
 261 calculated to reconstruct temperature changes during the past 4000 years (Fig. 4). The results
 262 indicate an overall trend of decreasing temperature; however, fluctuations in the abundance of
 263 cold-preference taxa indicate that the temperature was high in zone 1, decreased sharply
 264 around 2700 cal yr BP but maintained relatively high in zone 2, and fluctuated significantly
 265 and reached a minimum in zone 3. It is evident that the cold-preference taxa were more
 266 sensitive to temperature fluctuations and provide more detailed information about temperature
 267 variations than the warm-preference taxa, and thus changes in the abundance the former were
 268 primarily used to investigate temperature changes.

269 5.4 Wars and population changes

270 We calculated a total of 418 wars from 718 BC to 1911 AD. Given that the resolution of the
 271 Gonghai Lake samples ranges from 50-100 years, the incidences of wars were summed to



272 produce a 50 year-resolution. The cumulative frequency of these events is shown in Fig. 6c,
273 and was compared with the record of chironomid-inferred temperature variability (Fig. 6a)
274 and with the pollen-based precipitation reconstruction for Gonghai Lake (Fig. 6b; Chen et al.,
275 2015). The distribution of wars reveals that they occurred more frequently when temperature
276 and precipitation decreased abruptly, and they also lasted for a relatively long time (Fig. 6c).
277 For example, these events were the most severe during the LIA when both the temperature
278 and precipitation decreased significantly, which lasted for nearly 350 years. The results of
279 Pearson correlation and Granger causality analysis show that the change in abundance of the
280 cold-preference taxa are significantly related to the incidence of wars ($r=-0.189$ in Table 1,
281 $p<0.01$ in Table 2).

282 Only 19 records of population size in Shanxi Province since 340 BC are mentioned in Lu
283 and Teng (2006), and they were used in the present study. These data are evenly distributed
284 within each dynasty (Fig. 6d). Although the population size fluctuated significantly, an overall
285 increasing trend is evident, together with frequent population collapses following intervals
286 with a significant number of wars.

287

288

289 **Table 1**

290

291

292

293 **Table 2**

294

295



296 6 Discussion

297 6.1 Effects of temperature on the modern and fossil chironomids in Gonghai Lake 298 area

299 Although the fossil chironomid assemblages in Gonghai Lake mainly responded to changes in
300 EASM precipitation since the last deglaciation, the typical stenothermic taxa still responded
301 to temperature changes on various time scales (Wang et al., 2016). In the present study, the
302 results of RDA of modern chironomid assemblages and temperature variables (Fig. 3b), as
303 well as the Monte Carlo permutation test, demonstrate that TANN was a significant
304 environmental variable influencing the modern chironomid taxa. In addition, TANN has a
305 higher score on the first axes than the other variables in Fig. 3b, furthermore, TANN was the
306 only variable selected in the interactive-forward-selection ($p=0.026$). This result has rarely
307 been observed in the previous literature, although it has been noted that chironomids often
308 respond significantly to mean July or summer temperature (e.g., Brooks and Birks, 2001; Self
309 et al., 2011; Samartin et al., 2017). Our correlation between modern chironomid assemblages
310 and TANN provides a valuable reference for extracting temperature signals from the fossil
311 chironomid assemblages of Gonghai Lake. For example, *Chironomus gonghai*-type is ranked
312 at the end of the RDA of the modern assemblage data and TANN, indicating that it is
313 cold-temperature indicator in the Gonghai Lake region. Moreover, this taxon was abundant
314 during the YD, clearly indicating that it prefers a cold environment. However, *Chironomus* is
315 reported as a temperate indicator in chironomid records from Scotland and northern Russia
316 (e.g., Brooks et al., 2007; Brooks et al., 2012b; Nazarova et al., 2015). The reason for these
317 contradictory findings may be that *Chironomus gonghai*-type is a new species, or that
318 *Chironomus* has a different preference in the Gonghai Lake region. These observations
319 indicate that that it is necessary to improve the taxonomic resolution of chironomid



320 identifications and to establish more precisely the environmental preferences of chironomid
 321 taxa from local training sets to enhance the reliability of paleotemperature reconstructions.

322 6.2 Faunistics and inferred temperature change

323 Temperature variability in the Gonghai Lake region during the past 4000 years is clearly
 324 revealed by changes in the abundance of the cold-preference chironomid taxa (Fig. 4). The
 325 main reason for this may be that Gonghai is a high-elevation (1860 m a.s.l.) mountain lake
 326 and thus the mean annual water temperature is relatively low. The cold-preference taxa
 327 became dominant in Gonghai Lake and responded rapidly and sensitively to even minor
 328 temperature fluctuations. The decreasing trend of chironomid-inferred temperature is in
 329 accord with the variations in organic content of the Gonghai Lake sediments (Fig. 4). For lake
 330 sediments, the organic matter content perhaps reflects variations in organic productivity
 331 (Birks and Birks, 2006) and thus also probably reflects past regional temperature changes.
 332 However, other chironomid taxa in the Gonghai Lake record are indicators of temperate or
 333 cool, rather than cold, conditions. It is clearly important to determine whether they exhibit a
 334 similar trend of temperature change as the warm- and cold-preference taxa. Details of
 335 faunistics and inferred environmental change for each of the three intervals of the record are
 336 given below.

337 *4000-2700 cal yr BP.* During this interval, the temperate-preferring taxon *Cladotanytarsus*
 338 *mancus*-type (Brooks, 2006) is dominant. *Stictochironomus* and *Procladius*, which took a
 339 large percentage in this stage, respectively prefer an environment with temperatures $>12^{\circ}\text{C}$
 340 and $>10^{\circ}\text{C}$ in western Norway (Brooks and Birks, 2000). Thus, we infer that the temperature
 341 was relatively high during this interval.

342 *2700-1270 cal yr BP.* The abundance of the previously dominant warm-preference
 343 *Cladotanytarsus mancus*-type decreased abruptly and it was replaced by *Parakiefferiella*



344 *bathophila*-type which is also a warm-preference taxon (Brooks and Birks, 2000; Brooks,
 345 2000). This shift in the representation of the dominant warm-preference taxa probably
 346 occurred in the context of cold conditions, because the cold stenotherm *Hydrobaenus*
 347 *conformis*-type (Cranston et al., 1983) appears for the first time. In addition, another cold
 348 indicator, *Psectrocladius sordidellus*-type (Brooks and Heiri, 2013), also started to increase,
 349 marking the beginning of the 2700 cal yr BP cold event. However, the abundance of
 350 *Paratanytarsus penicillatus*-type, which is not usually indicative of cool temperatures, also
 351 increased since 2700 cal yr BP, simultaneously with *Psectrocladius sordidellus*-type. This
 352 curious combination of chironomid changes also occurred in a sediment record from
 353 Gerzensee, Switzerland (Brooks and Heiri, 2013). Overall, we infer that temperature began to
 354 decrease during this second stage

355 1270 cal yr BP-present. The cold-preference taxa, including *Hydrobaenus conformis*-type,
 356 *Psectrocladius sordidellus*-type and *Paratanytarsus penicillatus*-type, are dominant in this
 357 stage, while the relatively warm-preference taxa, including *Cladotanytarsus mancus*-type,
 358 *Parakiefferiella bathophila*-type and *Procladius*, exhibit low abundances. Thus, we conclude
 359 that temperatures reached a minimum. Several climatic events can be recognized; for example,
 360 chironomid subzones 3a, 3c and 3e correspond to the STWP, MWP and the modern warm
 361 period, respectively; in addition, subzones 3b and 3d correspond to the cold periods of the 5
 362 Dynasties & 10 Kingdoms in China and the LIA, respectively.

363 The foregoing analysis indicates that the temperature variability inferred by the
 364 characteristic of chironomid temperature-indicators is in accord with that inferred from the
 365 majority of other taxa in the Gonghai Lake sediments, suggesting that our methodology and
 366 results are reliable.

367 6.3 Intraregional temperature comparison



368 As mentioned previously, climate-model simulation results indicate that TANN in China was
369 higher in the late-Holocene than in the mid-Holocene (Jiang et al., 2012). In addition, even
370 the global TANN indicates a warming trend from the early Holocene onwards, due to the
371 retreating ice sheets and rising atmospheric greenhouse gas concentrations (Liu et al., 2014),
372 in contradiction to the cooling trend inferred from various proxy records for 30-90N (Marcott
373 et al., 2013). Our qualitative reconstruction of TANN in North China suggests that the
374 warming trend estimated for the late Holocene by the simulation results is not convincing.

375 To validate our chironomid-inferred temperature record (Fig. 5a), two unambiguous,
376 high-resolution, well-dated temperature reconstructions were chosen for comparison. The first
377 record is based on stalagmite layer thickness at Shihua Cave, close to Gonghai Lake (Tan et
378 al., 2003) (Fig. 5b); and the second is based on historical documents pertaining to winter
379 temperature changes in Eastern China (Ge et al., 2003) (Fig. 5c). The three records exhibit a
380 consistent pattern of temperature change on both a millennial and shorter scale: cold intervals
381 from 1350-1650 cal yr BP, 950-1150 cal yr BP and 300-650 cal yr BP (LIA); and warm
382 intervals from 1150-1350 cal yr BP (STWP) and 650-950 cal yr BP (MWP). In addition, a
383 single integrated temperature record for the whole of China was produced by combining
384 multiple paleoclimate proxy records from ice cores, tree rings, lake sediments and historical
385 documents (Fig. 5d, Yang et al., 2002) and was compared with the chironomid-inferred
386 temperature record from Gonghai Lake. Both records exhibit the same pattern of warm and
387 cold intervals during the past 2000 years: for example, the cold intervals of 1350-1650 cal yr
388 BP and 950-1150 cal yr BP, and the LIA, STWP, MWP and modern warm periods.

389 In addition to the consistency of the records described above, the trend of generally
390 decreasing temperature during the past 4000 years is also evident in several other recent
391 proxy-based reconstructions: for example, the U_{37}^K record from the sediments of Gahai and
392 Qinghai Lakes in the northeastern Tibetan Plateau (He et al., 2013; Wang et al., 2015), a novel



393 microbial lipid records from Dajiuhu in central China (Huang et al., 2013), percentages of
394 thermophilous trees in Huguangyan Maar Lake in southern China (Wang et al., 2007), and an
395 integrated temperature reconstruction for 30°-90° in the Northern Hemisphere (Fig. 5e)
396 (Marcott et al., 2013). The similarity of these proxy-based temperature reconstructions to a
397 record of total solar irradiance (Steinhilber et al., 2009; Fig. 5f) and the similar decreasing
398 trend of the various reconstructions and solar insolation (Berger and Loutre, 1991; Fig. 5g)
399 suggest that solar irradiance and insolation are important external drivers of temperature
400 variability during the late Holocene at centennial scale and millennial scale, respectively.

401 The foregoing demonstrates that our chironomid-based temperature reconstruction is
402 reliable and that the approach can be extended to longer time-scales. The success of our
403 approach can be attributed to the following factors: (i) Chironomids are sensitive to
404 temperature changes; (ii) the robust chronology increases the usefulness of the temperature
405 reconstruction; (iii) the precise high-resolution chronology enables the results to be compared
406 with documentary evidence and with other high-quality temperature reconstructions; and (iv)
407 the high-resolution record provides a detailed record of temperature changes. Furthermore,
408 our results, combined with a pollen-based precipitation reconstruction from the same core,
409 enable the identification of trends in both temperature and humidity (Fig. 6b, Chen et al.,
410 2015): for example, there were pronounced changes in warm-wet and cold-dry climatic
411 patterns on a millennial scale in the Gonghai Lake area, which is a monsoon-influenced
412 region. However, this pattern is not always evident on the centennial-scale: for example,
413 during 650-900 AD (Fig. 6) and 1650 AD-present (Fig. 6), the temperature was relatively high
414 while the precipitation was decreasing. This phenomenon is important for understanding
415 recent and ongoing climate change. In the past decade, many studies have attributed the
416 weakening of the Asian summer monsoon to anthropogenic aerosols in the atmosphere,
417 against the background of global warming (Menon et al., 2002; Bollasina et al., 2011; Yu et



al., 2016). However, decreasing precipitation in northern China associated with the weakening of the Asian summer monsoon (Liu et al., 2015) had also occurred during warm intervals during the past 1000 years. This inconsistency of changes in temperature and precipitation in the monsoonal region suggest that the recent weakening of the Asian summer monsoon may not only be the result of anthropogenic aerosols, but also be due to natural variability.

Figure 5

6.4 Relationship between societal crises in Shanxi Province and climate change

Although past wars in China were often the consequence of social-geopolitical factors, including territorial disputes (Zhao, 2006), nomadic invasions, and agricultural expansion (Di Cosmo, 2002), the impact of climate change should also be considered when analyzing societal evolution (Ge, 2011). Traditionally, China was an agricultural society the productivity of which was very low during most of its history. When temperature or precipitation decreased abruptly, or fluctuated significantly, there tended to be an increase in the incidence of natural disasters such as floods and droughts (Zhang et al., 2008) which seriously affected agricultural production. The combination of a large population and a poor grain harvest often resulted in high rice prices, famines, generating large numbers of homeless refugees and plague. These factors would finally trigger wars and social unrest which acted to reduce the population size. To analyze the societal response in Shanxi Province to climate change, the occurrence of wars (Fig. 6c) and changes in population size (Fig. 6d) were summarized for comparison with the chironomid-inferred temperature record (Fig. 6a) and the pollen-based



442 precipitation reconstruction (Fig. 6b; Chen et al., 2015) from Gonghai Lake.

443 Although both temperature and precipitation in the Gonghai Lake region exhibit a
444 decreasing trend during the last 4000 years, temperature changes were not always in phase
445 with precipitation changes. For example, four cold events can be recognized from the
446 chironomid-inferred temperature record (Fig. 6a), which occurred during ~760-230 BC
447 (Spring & Autumn and Warring States Period), 260-650 AD (Era of Disunity), 900-1050 AD
448 (5 Dynasties and 10 Kingdoms), and 1300-1650 AD (Ming Dynasty). The reconstructed
449 precipitation record only exhibits two dry events during this interval, from ~900-1050 AD and
450 from 1300-1650 AD. The societal response to such events varied during different periods. The
451 incidence of war was especially high during 900-1050 AD and 1300-1650 AD when both
452 temperature and precipitation were lower; it was higher at these times than during the periods
453 of 760-230 BC and 260-600 AD when only temperature was lower. This relationship is
454 confirmed by the results of Granger causality analysis (see Table 2 in *War and population*),
455 which show that the incidence of wars is more strongly correlated with temperature changes
456 than with precipitation. However, this may only be a statistical artifact and the causal
457 relationship between climate change and societal crises needs to be further tested in future
458 research. A sharp decrease in temperature may have been an important precondition for an
459 outbreak of war in China, but it may have insufficient in isolation, and decreases in
460 precipitation during the past 3000 years may also have been important. Moreover, the fact that
461 historical documents in China became increasingly detailed and reliable as human society
462 developed (Ge et al., 2010) may be an additional explanation for the observation that
463 increases in the frequency of wars persistently coincided with decreases in temperature and
464 precipitation. With regard to population, an increase often occurred during warm periods
465 which would have created latent economic pressures when the crop harvest was poor
466 following a cold period. In addition, population collapse often occurred following an increase



467 in the frequency of wars during cold periods, suggesting that population size was significantly
 468 influenced by climate change.

469 The demise of the Ming dynasty provides an example of how climatic deterioration, as well
 470 as the related socioeconomic impacts, severely undermined an empire in historical China. The
 471 late Ming (1560-1644 AD) coincided with the Little Ice Age, when temperatures decreased
 472 significantly (Fig. 6a). During this cold period, the incidence of natural disasters such as flood
 473 and droughts was the highest in Shanxi history (Chen, 1939). Rapid cooling accompanied by
 474 large-scale desertification began in the 1620s and had a devastating effect on agricultural
 475 production (Wang et al., 2010; Yin et al., 2015). Zheng *et al.* (2014) noted that the total grain
 476 yield in Shanxi in the 1630s ranged from 1219.8×10^6 to 1951.3×10^6 kg, a reduction of almost
 477 50 % compared to the yield of ~1580 (2439.1×10^6 kg). The population increased from 8.42 to
 478 9.50 million throughout this period (Zheng et al., 2014) and it seemed that widespread
 479 famines would be unavoidable given the additional factor that governmental disaster relief
 480 malfunctioned due to political corruption in the late Ming (Zheng et al., 2014; Xiao et al.,
 481 2015). Furthermore, the fiscal situation of the Ming was precarious since conflicts with the
 482 Jurchen people soon exhausted the treasury and the government was forced to levy higher
 483 taxes on the peasants (Huang, 1974; Gu, 1984; Wei et al., 2014). The exacerbation of the food
 484 crisis consequently triggered a prolonged peasant uprising which broke out in northern
 485 Shaanxi, spread to Shanxi, and finally overturned the Ming Empire in 1644. The historical
 486 records at a provincial level are voluminous and the socioeconomic context was complex and
 487 further research is needed regarding the relationship between climate change and the societal
 488 response on a regional scale in China

489

490

491

Figure 6



492 -----

493

494 7 Conclusions

495 Chironomids are a stenotypic and sensitive temperature proxy. Together with a robust
 496 chronology and modern calibration set, we used chironomid assemblages from the sediments
 497 of Gonghai Lake to reconstruct temperature variations during the past 4000 years in northern
 498 China. Combined with historical documents, the temperature record was used to explore the
 499 relationship between climate change and human societal changes at the regional scale. The
 500 principal conclusions are as follows:

501 (1) The chironomid-inferred temperature record exhibits a stepwise decreasing trend since
 502 4000 cal yr BP. Temperature remained high during 4000-2700 cal yr BP; decreased abruptly
 503 around 2700 cal yr BP; decreased gradually from 2700-1270 cal yr BP; and reached a
 504 minimum, accompanied by frequent fluctuations during the last 1270 years. In addition, the
 505 cold events, corresponding to the Era of Disunity in China, the STWP, MWP and LIA,
 506 revealed in the chironomid record from Gonghai Lake were also recorded in numerous other
 507 multi-proxy records, indicating that our temperature reconstruction is reliable and
 508 representative.

509 (2) The frequency of wars in Shanxi Province during the last 2700 years is significantly
 510 correlated with the chironomid-inferred temperature record from Gonghai Lake. Reductions
 511 in population size, associated with warfare and famine, are also correlated with the
 512 temperature fluctuations. We suggest that the impacts of temperature and precipitation on
 513 human society should be further studied in the future.

514

515 **Acknowledgements.** We thank Qiang Wang and Haichao Xie for help with fieldwork, Prof.



516 Guanghui Dong and Dr. Harry F. Lee for helpful discussions, and Dr. Jan Bloemendal for
517 English editing. This research was jointly supported by the National Natural Science
518 Foundation of China (41471162) and the National Key R&D Program of China
519 (2017YFA0603402).



520 **References:**

- 521 Berger, A. and Loutre, M.F.: Insolation values for the climate of the last 10 million years, *Quat. Sci.*
522 *Rev.*, 10(4), 297-317, 1991.
- 523 Birks, H.H. and Birks, H.J.B.: Multi-proxy studies in palaeolimnology, *Veg. Hist. Archaeobot.*, 15,
524 235-251, 2006.
- 525 Bollasina, M.A., Ming, Y., and Ramaswamy, V.: Anthropogenic aerosols and the weakening of the
526 South Asian summer monsoon, *Science*, 334, 502-505, 2011.
- 527 Brodin, Y.W.: The postglacial history of Lake Flarken, southern Sweden, interpreted from subfossil
528 insect remains, *Int. Rev. Hydrobiol.*, 71, 371-432, 1986.
- 529 Brooks, S.J.: Late-glacial fossil midge stratigraphies (Insecta: Diptera: Chironomidae) from the Swiss
530 Alps, *Palaeogeogr. Palaeoclimatol. Palaeoecol.*, 159(3), 261-279, 2000.
- 531 Brooks, S.J.: Chironomidae (Insecta: Diptera), In: MacKay A, Battarbee RW, Birks HJB, (Eds) *Global*
532 *change in the Holocene* Arnold, London, 2003.
- 533 Brooks, S.J.: Fossil midges (Diptera: Chironomidae) as palaeoclimatic indicators for the Eurasian
534 region, *Quat. Sci. Rev.*, 25, 1894-1910, 2006.
- 535 Brooks, S.J., Axford, Y., Heiri, O., Langdon, P.G., and Larocque-Tobler I.: Chironomids can be reliable
536 proxies for Holocene temperatures. A comment on Velle et al. (2010), *Holocene*, 22(12), 1495-1500,
537 2012a.
- 538 Brooks, S.J. and Birks, H.J.B.: Chironomid-inferred late-glacial and early-Holocene mean July air
539 temperatures for Kråkenes Lake, western Norway, *J. Paleolimnol.*, 23(1), 77-89, 2000.
- 540 Brooks, S.J. and Birks, H.J.B.: Chironomid-inferred air temperatures from Lateglacial and Holocene
541 sites in north-west Europe: progress and problems, *Quat. Sci. Rev.*, 20(16), 1723-1741, 2001.
- 542 Brooks, S.J. and Heiri, O.: Response of chironomid assemblages to environmental change during the
543 early Late-glacial at Gerzensee, Switzerland, *Palaeogeogr. Palaeoclimatol. Palaeoecol.*, 391, 90-98,
544 2013.
- 545 Brooks, S.J., Langdon, P.G., and Heiri, O.: The identification and use of Palaearctic Chironomidae
546 larvae in palaeoecology, *Quaternary Research Association*, London, 2007.
- 547 Brooks, S.J., Matthews, I.P., Birks, H.H., and Birks, H.J.B.: High resolution Lateglacial and
548 early-Holocene summer air temperature records from Scotland inferred from chironomid assemblages,
549 *Quat. Sci. Rev.*, 41, 67-82, 2012b.
- 550 Chen, F.H., Xu, Q.H., Chen, J.H., Birks, H.J.B., Liu, J.B., Zhang, S.R., Jin, L.Y., An, C.B., Telford, R.J.,



- 551 Cao, X.Y., Wang, Z.L., Zhang, X.J., Selvaraj, K., Lü, H.Y., Li, Y.C., Zheng, Z., Wang, H.P., Zhou, A.F.,
552 Dong, G.H., Zhang, J.W., Huang, X.Z., Bloemendal, J., and Rao, Z.G.: East Asian summer monsoon
553 precipitation variability since the last deglaciation, *Sci. Rep.*, doi: <http://dx.doi.org/10.1038/srep11186>,
554 2015.
- 555 Chen, G.Y.: China successive natural and manmade disasters table (in Chinese), Jinan University Book
556 Series, Guangzhou, 1939.
- 557 Chen, J.H., Chen, F.H., Zhang, E.L., Brooks, S.J., Zhou, A.F., and Zhang, J.W.: A 1000-year
558 chironomid-based salinity reconstruction from varved sediments of Sugan Lake, Qaidam Basin, arid
559 Northwest China, and its palaeoclimatic significance, *Chin. Sci. Bull.*, 54(20), 3749-3759, 2009.
- 560 Chen, J.H., Rao, Z.G., Liu, J.B., Huang, W., Feng, S., Dong, G.H., Hu, Y., Xu, Q.H., and Chen, F.H.:
561 On the timing of the East Asian summer monsoon maximum during the Holocene—Does the
562 speleothem oxygen isotope record reflect monsoon rainfall variability?, *Sci. China Ser. D Earth Sci.*, 59,
563 2328-2338, 2016.
- 564 Chen, J.H., Zhang, E.L., Brooks, S.J., Huang, X.Z., Wang, H.P., Liu, J.B., and Chen, F.H.:
565 Relationships between chironomids and water depth in Bosten Lake, Xinjiang, northwest China, *J.*
566 *Paleolimnol.*, 51(2), 313-323, 2014.
- 567 Cranston, P.S., Oliver, D.R., and Saether, O.A.: The larvae of Orthocladiinae (Diptera: Chironomidae)
568 of the Holarctic region: keys and diagnoses, *Ent. scand. Suppl.*, 19, 149-291, 1983.
- 569 Di Cosmo, N.: Ancient China and its enemies: The rise of nomadic power in East Asian history,
570 Cambridge University Press, 2002.
- 571 Dykoski, C.A., Edwards, R.L., Cheng, H., Yuan, D.X., Cai, Y.J., Zhang, M.L., Lin, Y.S., Qing, J.M., An,
572 Z.S., and Revenaugh, J.: A high-resolution, absolute-dated Holocene and deglacial Asian monsoon
573 record from Dongge Cave, China, *Earth Planet Sci. Lett.*, 233, 71-86, 2005.
- 574 Editorial Committee of Chinese Military History: Tabulation of Wars in Ancient China (in Chinese),
575 People's Liberation Army Press, Beijing, 1985.
- 576 Eggermont, H., Heiri, O., Russell, J., Vuille, M., Audenaert, L., and Verschuren, D.: Paleotemperature
577 reconstruction in tropical Africa using fossil Chironomidae (Insecta: Diptera), *J. Paleolimnol.*, 43(3),
578 413-435, 2010.
- 579 Gao, L., Nie, J.S., Clemens, S., Liu, W.G., Sun, J.M., Zech, R., and Huang, Y.S.: The importance of
580 solar insolation on the temperature variations for the past 110 kyr on the Chinese Loess Plateau,
581 *Palaeogeogr. Palaeoclimatol. Palaeoecol.*, 317-318 (1), 128-133, 2012.
- 582 Ge, Q.S.: Climate change in Chinese dynasties, Science Press, Beijing, China, 2011.



- 583 Ge, Q.S., Zheng, J.Y., Fang, X.Q., Man, Z.M., Zhang, X.Q., Zhang, P.Y., and Wang, W.C.: Winter
584 half-year temperature reconstruction for the middle and lower reaches of the Yellow River and Yangtze
585 River, China, during the past 2000 years, *Holocene*, 13(6), 933-940, 2003.
- 586 Ge, Q.S., Zheng, J.Y., Hao, Z.X., Shao, X.M., Wang, W.C., and Luterbacher, J.: Temperature variation
587 through 2000 years in China: An uncertainty analysis of reconstruction and regional difference,
588 *Geophys. Res. Lett.*, 37(3), 2010.
- 589 Grimm, E.C.: *Tilia and Tilia. Graph v. 2.0.2*, Illinois State Museum, Springfield, USA, 2004.
- 590 Gu, C.: *History of Peasant Wars in the End of the Ming Dynasty* (in Chinese), Social Sciences Press,
591 Beijing, China, 1984.
- 592 He, Y.X., Liu, W.G., Zhao, C., Wang, Z., Wang, H.Y., Liu, Y., Qin, X.Y., Hu, Q.H., An, Z.S., and Liu,
593 Z.H.: Solar influenced late Holocene temperature changes on the northern Tibetan Plateau, *Chin. Sci.*
594 *Bull.*, 58(9), 1053-1059, 2013.
- 595 Heiri, O., Brooks, S.J., Birks, H.J.B., and Lotter, A.F.: A 274-lake calibration data-set and inference
596 model for chironomid-based summer air temperature reconstruction in Europe, *Quat. Sci. Rev.*,
597 30(23-24), 3445-3456, 2011.
- 598 Heiri, O., Lotter, A.F., and Lemcke, G.: Loss on ignition as a method for estimating organic and
599 carbonate content in sediments: reproducibility and comparability of results, *J. Paleolimnol.*, 25,
600 101-110, 2001.
- 601 Huang, R.: *Taxation and governmental finance in sixteenth-century Ming China* (Vol. 4), Cambridge
602 University Press, 1974.
- 603 Huang, X.Y., Meyers, P.A., Jia, C.L., Zheng, M., Xue, J.T., Wang, X.X., and Xie, S.C.:
604 Paleotemperature variability in central China during the last 13 ka recorded by a novel microbial lipid
605 proxy in the Dajihu peat deposit, *Holocene*, 23(8), 1123-1129, 2013.
- 606 Jia, G.D., Rao, Z.G., Zhang, J., Li, Z.Y., and Chen, F.H.: Tetraether biomarker records from a
607 loess-paleosol sequence in the western Chinese Loess Plateau, *Front. Microbiol.*, 4, 199, 2013.
- 608 Jiang, D.B., Lang, X.M., Tian, Z.P., and Wang, T.: Considerable Model-Data Mismatch in Temperature
609 over China during the Mid-Holocene: Results of PMIP Simulations, *J. Clim.*, 25, 4135-4153, 2012.
- 610 Levesque, A.J., Cwynar, L.C., and Walker, I.R.: Exceptionally steep north-south gradients in lake
611 temperatures during the last deglaciation, *Nature*, 385(423-426), 1997.
- 612 Liu, J.B., Chen, J.H., Zhang, X.J., Li, Y., Rao, Z.G., and Chen, F.H.: Holocene East Asian summer
613 monsoon records in northern China and their inconsistency with Chinese stalagmite $\delta^{18}\text{O}$ records, *Earth*
614 *Sci. Rev.*, 148, 194-208, 2015.



- 615 Liu, Z., Zhu, J., Rosenthal, Y., Zhang, X., Otto-Bliesner, B.L., Timmermann, A., Smith, R.S., Lohmann,
616 G., Zheng, W.P., and Timm, O.E.: The Holocene temperature conundrum, *Proc. Natl. Acad. Sci. U.S.A.*,
617 111(34), 3501-3505, 2014.
- 618 Liu, J.B., Chen, S.Q., Chen, J.H., Zhang, Z.P., and Chen, F.H.: Chinese cave $\delta^{18}\text{O}$ records do not
619 represent northern East Asian summer monsoon rainfall, *Proc. Natl. Acad. Sci. U.S.A.*, 201703471,
620 2017.
- 621 Lu, Y. and Teng, Z.: *Zhongguo Fenshengqu Lishi Renkou Kao* (Examination of historical Chinese
622 population in various provinces and districts), Shandong Renmin Chubanshe, Jinan Shi, 2006.
- 623 Marcott, S.A., Shakun, J.D., Clark, P.U., Clark, P.U., and Mix, A.C.: A reconstruction of regional and
624 global temperature for the past 11,300 years, *Science*, 339(6124), 1198-1201, 2013.
- 625 Massferro, J. and Larocque-Tobler, I.: Using a newly developed chironomid transfer function for
626 reconstructing mean annual air temperature at Lake Potrok Aike, Patagonia, Argentina, *Ecol. Indic.*,
627 24(1), 201-210, 2013.
- 628 Menon, S., Hansen, J., Nazarenko, L., and Luo, Y.: Climate effects of black carbon aerosols in China
629 and India, *Science*, 297, 2250-2253, 2002.
- 630 Nazarova, L., Herzsuh, U., Wetterich, S., Kumke, T., and Pestryakova, L.: Chironomid-based
631 inference models for estimating mean July air temperature and water depth from lakes in Yakutia,
632 northeastern Russia, *J. Paleolimnol.*, 45(1), 57-71, 2011.
- 633 Nazarova, L., Self, A.E., Brooks, S.J., van Hardenbroek, M., Herzsuh, U., and Diekmann, B.:
634 Northern Russian chironomid-based modern summer temperature data set and inference models, *Glob.*
635 *Planet Change*, 134, 10-25, 2015.
- 636 Peterse, F., Martínez-García, A., Zhou, B., Beets, C.J., Prins, M.A., Zheng, H.B., and Eglinton, T.I.:
637 Molecular records of continental air temperature and monsoon precipitation variability in East Asia
638 spanning the last 130,000 years, *Quat. Sci. Rev.*, 83, 76-82, 2014.
- 639 Peterse, F., Prins, M.A., Beets, C.J., Troelstra, S.R., Zheng, H.B., Gu, Z.Y., Schouten, S., and Damsté
640 J.S.S.: Decoupled warming and monsoon precipitation in East Asia over the last deglaciation, *Earth*
641 *Planet Sci. Lett.*, 301, 256-264, 2011.
- 642 R Core Team: R: A language and environment for statistical computing, R Foundation for Statistical
643 Computing, Vienna, Austria, 2013, 2014.
- 644 Rees, A.B.H., Cwynar, L.C., and Cranston, P.S.: Midges (Chironomidae, Ceratopogonidae,
645 Chaoboridae) as a temperature proxy: a training set from Tasmania, Australia, *J. Paleolimnol.*, 40(4),
646 1159-1178, 2008.



- 647 Reimer, P.J., Baillie, M.G.L., Bard, E., Bayliss, A., Beck, J.W., Blackwell, P.G., Ramsey, C.B., Buck,
648 C.E., Burr, G.S., Edwards, R., Friedrich, M., Grootes, P.M., Guilderson, T.P., Hajdas, I., Heaton, T.J.,
649 Hogg, A.G., Hughen, K.A., Kaiser, K.F., Kromer, B., McCormac, F.G., Manning, S.W., Reimer, R.W.,
650 and Richards, D.A.: Intcal09 and Marine09 radiocarbon age calibration curves 0-50,000 years cal BP,
651 Radiocarbon, 51(4), 1111-1150, 2009.
- 652 Rieradevall, M. and Brooks, S.J.: An identification guide to subfossil Tanypodinae larvae (Insecta:
653 Diptera: Chironomidae) based on cephalic setation, J. Paleolimnol., 23, 81-99, 2001.
- 654 Samartin, S., Heiri, O., Joos, F., Renssen, H., Franke, J., Brönnimann, S., and Tinner, W.: Warm
655 Mediterranean mid-Holocene summers inferred from fossil midge assemblages, Nat. Geosci., 10(3),
656 207-212, 2017.
- 657 Self, A.E., Brooks, S.J., Birks, H.J.B., Nazarova, L., Porinchu, D., Odland, A., Yang, H., and Jones, V.J.:
658 The distribution and abundance of chironomids in high-latitude Eurasian lakes with respect to
659 temperature and continentality: development and application of new chironomid-based
660 climate-inference models in northern Russia, Quat. Sci. Rev., 30(9), 1122-1141, 2011.
- 661 Shi, Y.F., Kong, Z.C., Wang, S.M., Tang, L.Y., Wang, F.B., Yao, T.D., Zhao, X.T., Zhang, P.Y., and Shi,
662 S.H.: Mid-Holocene climates and environments in China, Glob. Planet Change, 7(1-3), 219-233, 1993.
- 663 Steinhilber, F., Beer, J., and Fröhlich, C.: Total solar irradiance during the Holocene, Geophys. Res.
664 Lett., 36(19), 308-308, 2009.
- 665 Stocker, T.F., Qin, D.H., Plattner, G.K., Tignor, M.M.B., Allen, S.K., Boschung, J., Nauels, A., Xia, Y.,
666 Bex, V., and Midgley, P.M.: Climate Change 2013: The Physical Science Basis. Contribution of
667 Working Group I to the Fifth Assessment Report of the Intergovernmental Panel on Climate Change,
668 Cambridge University Press, doi: 10.1017/CBO9781107415324, Cambridge, 2013.
- 669 Tan, M., Liu, T.S., Hou, J.Z., Qin, X.G., Zhang, H.C., and Li, T.Y.: Cyclic rapid warming on
670 centennial-scale revealed by a 2650-year stalagmite record of warm season temperature, Geophys. Res.
671 Lett., 30(12), 2003.
- 672 Walker, I.R.: Midges: Chironomidae and related Diptera. In: Smol, J.P., Birks, H.J.B., Last, W.M.
673 (Eds.), Tracking Environmental Change Using Lake Sediments, Kluwer Academic Publishers,
674 Dordrecht, 43-66, 2001.
- 675 Walker, I.R.: The WWW Field Guide to Fossil Midges (<http://www.paleolab.ca/wwwguide/>), 2007.
- 676 Walker, I.R. and Cwynar, L.C.: Midges and palaeotemperature reconstruction—the North American
677 experience, Quat. Sci. Rev., 1911-1925, 2006.
- 678 Walker, I.R., Mott, R.J., and Smol, J.P.: Allerød-Younger Dryas Lake Temperatures from Midge Fossils
679 in Atlantic Canada, Science, 253(5023), 1010, 1991.



- 680 Wang, H.P., Brooks, S.J., Chen, J.H., Hu, Y., Wang, Z.L., Liu, J.B., Xu, Q.H., and Chen, F.H.:
681 Response of chironomid assemblages to East Asian summer monsoon precipitation variability in
682 northern China since the last deglaciation, *J. Quat. Sci.*, 31(8), 967-982, 2016.
- 683 Wang, S., Gong, D., and Zhu, J.: Twentieth-century climatic warming in China in the context of the
684 Holocene, *Holocene*, 11(3), 313-321, 2001.
- 685 Wang, S.Y., Lü H.Y., Liu, J.Q., and Jörg, F.W.N.: The early Holocene optimum inferred from a
686 high-resolution pollen record of Huguangyan Maar Lake in southern China, *Chin. Sci. Bull.*, 52(20),
687 2829-2836, 2007.
- 688 Wang, X., Chen, F., Zhang, J., Yang, Y., Li, J., Hasi, E., Zhang, C., and Xia, D.: Climate, desertification,
689 and the rise and collapse of China's historical dynasties, *Hum. Ecol.*, 38(1), 157-172, 2010.
- 690 Wang, X., Wang, Z.L., Chen, J.H., Liu, J.B., Wang, H.P., Xu, Q.H., Zhang, S.R., and Chen, F.H.: On
691 the origin of the upland lake group in Ningwu Tianchi region, Shanxi Province (in Chinese with
692 English abstract), *Journal of Lanzhou University (Natural Sciences)*, 50, 208-212, 2014.
- 693 Wang, Z., Liu, Z., Zhang, F., Fu, M.Y., and An, Z.S.: A new approach for reconstructing Holocene
694 temperatures from a multi-species long chain alkenone record from Lake Qinghai on the northeastern
695 Tibetan Plateau, *Org. Geochem.*, 88, 50-58, 2015.
- 696 Watson, J.E., Brooks, S.J., Whitehouse, N.J., Reimer, P.J., Birks, H.J.B., and Turney, C.:
697 Chironomid-inferred late-glacial summer air temperatures from Lough Nadourcan, Co. Donegal,
698 Ireland, *J. Quat. Sci.*, 25(8), 1200-1210, 2010.
- 699 Wei, Z., Fang, X., and Su, Y.: Climate change and fiscal balance in China over the past two millennia,
700 *Holocene*, 24(12), 1771-1784, 2014.
- 701 Wen, R.L., Xiao, J.L., Chang, Z.G., Zhai, D.Y., Xu, Q.H., Li, Y.C., and Itoh, S.: Holocene precipitation
702 and temperature variations in the East Asian monsoonal margin from pollen data from Hulun Lake in
703 northeastern Inner Mongolia, China, *Boreas*, 39(2), 262-272, 2010.
- 704 Wiederholm, T.E.: Chironomidae of the Holarctic region. Keys and diagnoses. Part 1. Larvae, *Ent.*
705 *scand. Suppl.*, 19, 1-457, 1983.
- 706 Xiao, L., Fang, X., Zheng, J., and Zhao, W.: Famine, migration and war: Comparison of climate change
707 impacts and social responses in North China between the late Ming and late Qing dynasties, *Holocene*,
708 25(6), 900-910, 2015.
- 709 Xu, Q.H., Xiao, J.L., Li, Y.C., Tian, F., and Nakagawa, T.: Pollen-based quantitative reconstruction of
710 Holocene climate changes in the Daihai Lake area, Inner Mongolia, China, *J. Clim.*, 23(11), 2856-2868,
711 2010.



- 712 Yang, B., Braeuning, A., Johnson, K.R., and Shi, Y.F.: General characteristics of temperature variation
713 in China during the last two millennia, *Geophys. Res. Lett.*, 29(9), 2002.
- 714 Yin, J., Su, Y., and Fang, X.Q.: Relationships between temperature change and grain harvest
715 fluctuations in China from 210 BC to 1910 AD, *Quat. Int.*, 355, 153-163, 2015.
- 716 Yu, S.C., Li, P.F., Wang, L.Q., Wang, P., Wang, S., Chang, S.C., Liu, W.P., and Alapaty, K.:
717 Anthropogenic aerosols are a potential cause for migration of the summer monsoon rain belt in China,
718 *Proc. Natl. Acad. Sci. U.S.A.*, 113, E2209-E2210, 2016.
- 719 Zhang, D.D., Jim, C.Y., Lin, C.S., He, Y.Q., and Lee, H.F.: Climate change, social unrest and dynastic
720 transition in ancient China, *Chin. Sci. Bull.*, 50(2), 137-144, 2005.
- 721 Zhang, D.D., Lee, H.F., Wang, C., Li, B.S., Pei, Q., Zhang, J., and An, Y.L.: The causality analysis of
722 climate change and large-scale human crisis, *Proc. Natl. Acad. Sci. U.S.A.*, 108(42), 17296-17301,
723 2011.
- 724 Zhang, D.D., Pei, Q., Lee, H.F., Zhang, J., Chang, C.Q., Li, B., Li, J., and Zhang, X.: The pulse of
725 imperial China: A quantitative analysis of long-term geopolitical and climatic cycles, *Glob. Ecol.*
726 *Biogeogr.*, 24(1), 87-96, 2015.
- 727 Zhang, E.L., Bedford, A., Jones, R., Shen, J., Wang, S.M., and Tang, H.Q.: A subfossil chironomid-total
728 phosphorus inference model for lakes in the middle and lower reaches of the Yangtze River, *Chin. Sci.*
729 *Bull.*, 51(17), 2125-2132, 2006.
- 730 Zhang, E.L., Chang, J., Cao, Y.M., Tang, H.Q., Langdon, P., Shulmeister, J., Wang, R., Yang, X.D., and
731 Shen, J.: A chironomid-based mean July temperature inference model from the south-east margin of the
732 Tibetan Plateau, China, *Clim. Past*, 13, 185-199, 2017a.
- 733 Zhang, E.L., Chang, J., Cao, Y.M., Su, W.W., Shulmeister, J., Tang, H.Q., Langdon, P., Yang, X.D., and
734 Shen, J.: Holocene high-resolution quantitative summer temperature reconstruction based on subfossil
735 chironomids from the southeast margin of the Qinghai-Tibetan Plateau, *Quat. Sci. Rev.*, 165, 1-12,
736 2017b.
- 737 Zhang, E.L., Jones, R., Bedford, A., Langdon, P., and Tang, H.: A chironomid-based salinity inference
738 model from lakes on the Tibetan Plateau, *J. Paleolimnol.*, 38(4), 477-491, 2007.
- 739 Zhang, Q., Gemmer, M., and Chen, J.: Climate changes and flood/drought risk in the Yangtze Delta,
740 China, during the past millennium, *Quat. Int.*, 176, 62-69, 2008.
- 741 Zhao, D.X.: Warfare in Eastern Zhou and the Rise of Confucian-Legal State (in Chinese), East China
742 Normal University Press, Shanghai, 2006.
- 743 Zhao, Y., Chen, F.H., Zhou, A.F., Yu, Z.C., and Zhang, K.: Vegetation history, climate change and



- 744 human activities over the last 6200 years on the Liupan Mountains in the southwestern Loess Plateau in
745 central China, *Palaeogeogr. Palaeoclimatol. Palaeoecol.*, 293(1), 197-205, 2010.
- 746 Zheng, J.Y., Xiao, L.B., Fang, X.Q., Hao, Z.X., Ge, Q.S., and Li, B.B.: How climate change impacted
747 the collapse of the Ming dynasty, *Clim. Change*, 127(2), 169-182, 2014.



748 **Table captions**

749 **Table 1** Results of Pearson correlation analysis of cold-preference chironomid taxa percentages,
750 reconstructed precipitation and incidence of war.

751 **Table 2** Granger causality analysis of cold-preference chironomid taxa percentages, reconstructed
752 precipitation and incidence of war.



753 **Table 1**

		War
Cold Taxa	Pearson correlation (r)	0.571**
	Significance (p)	0.000
Precipitation	Pearson correlation (r)	-0.214
	Significance (p)	0.125

754 **. p<0.01 (2-tailed).

755

756 **Table 2**

Null Hypothesis	F	p
COLD TAXA do not Granger Cause WAR	16.4887	0.0002**
PRECIPITATION does not Granger Cause WAR	0.96106	0.3317

757 **. p<0.01.



758 **Figure captions**

759 **Figure 1** (a) Location of Gonghai Lake (blue dot) and other temperature records in North China. (b)
 760 Location of sediment core GH09B.

761 **Figure 2** Age-depth model for core GH09B (modified from Chen et al., 2015).

762 **Figure 3** Information about the modern calibration data set obtained from the Gonghai Lake area. (a)
 763 Location of modern surface samples (white dots); (b) RDA bi-plot of modern chironomid assemblages
 764 and TANN, summer Tem, June Tem, July Tem and August Tem; and (c) relative abundance of modern
 765 chironomid assemblages from the modern calibration set (Wang et al., 2016). All taxa are arranged
 766 according to their RDA 1 scores of chironomids and TANN. Only taxa occurring in at least two
 767 samples with an abundance of >2 % are plotted.

768 **Figure 4** Relative abundance of the main chironomid taxa from Gonghai Lake during the past 4000
 769 years. Taxa are plotted from left to right in order of their DCA 1 scores. Loss-on-ignition (LOI) values,
 770 chironomid concentration, percentages of warm- and cold-preference taxa are plotted as red lines with
 771 squares, black bars, and red and blue patterns, respectively. Three chironomid assemblage zones were
 772 defined by CONISS results.

773 **Figure 5** Comparison of (a) cold-preference taxa percentages in Gonghai Lake with intraregional
 774 temperature records during the past 4000 years, including (b) reconstructed temperature based on
 775 stalagmite layer thickness in Shihua Cave (Tan et al., 2003), (c) winter half-year temperature anomalies
 776 in eastern China with a 30-year resolution (Ge et al., 2003), (d) weighted temperature reconstruction
 777 for China obtained by combining multiple paleoclimate proxy records (Yang et al., 2002), (e) and the
 778 paleotemperature for 30 °–90 ° of the North Hemisphere (Marcott et al., 2013). All the temperature
 779 records are compared with (f) a reconstruction of total solar irradiance (Steinhilber et al., 2009) and
 780 summer insolation at 65 °N (Berger and Loutre, 1991) during the past 4000 years. Grey shaded areas
 781 indicate cold periods.

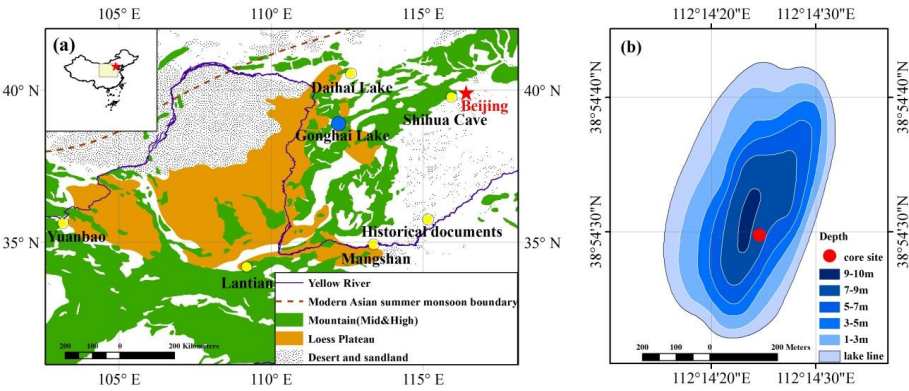
782 **Figure 6** Comparison of (a) cold taxa percentages and (b) reconstructed precipitation at Gonghai Lake



783 (Chen et al., 2015) with (c) frequencies of wars in Shanxi Province, China and (d) population size (in
784 units of 1 million, square dots) of Shanxi Province during the past 2300 years; the data are spline
785 connected. Grey shaded areas indicate abrupt temperature decreases.



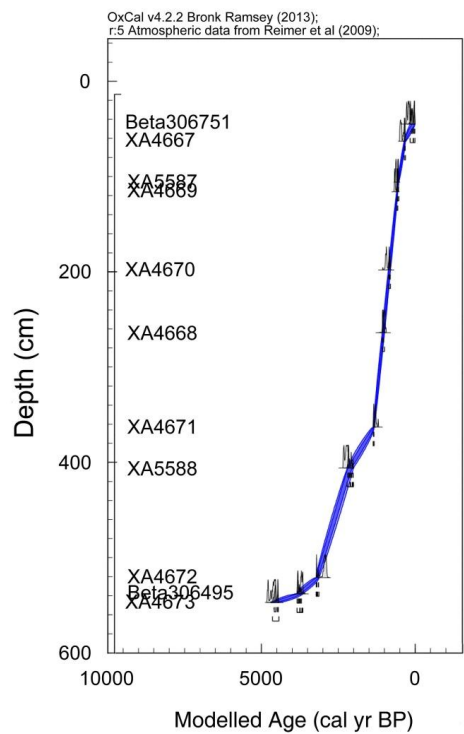
786 **Fig. 1**



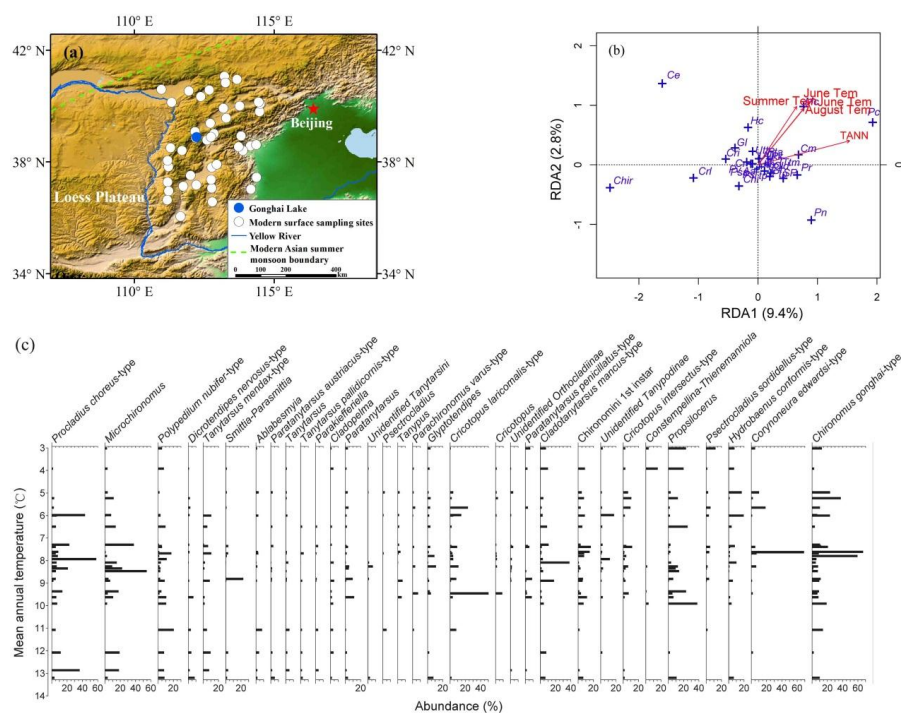
787

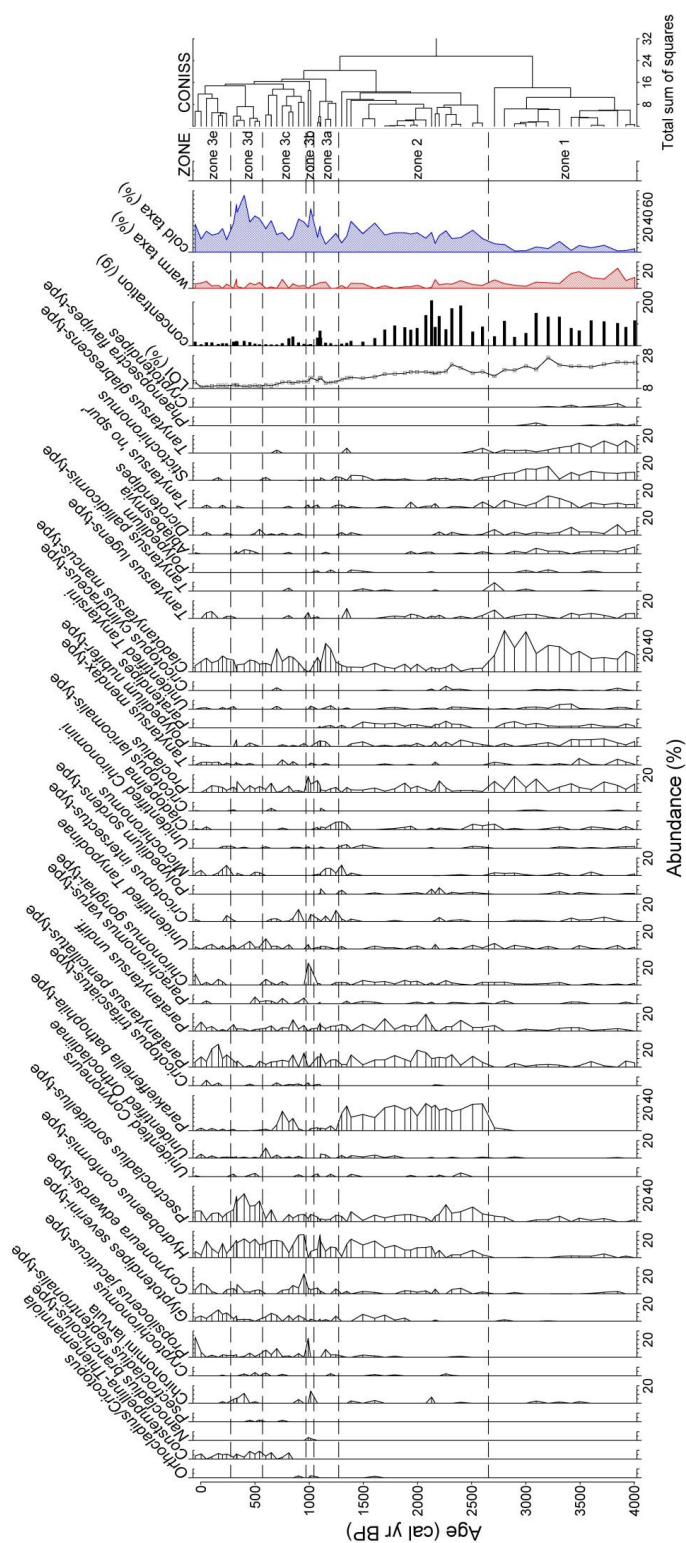


788 **Fig. 2**



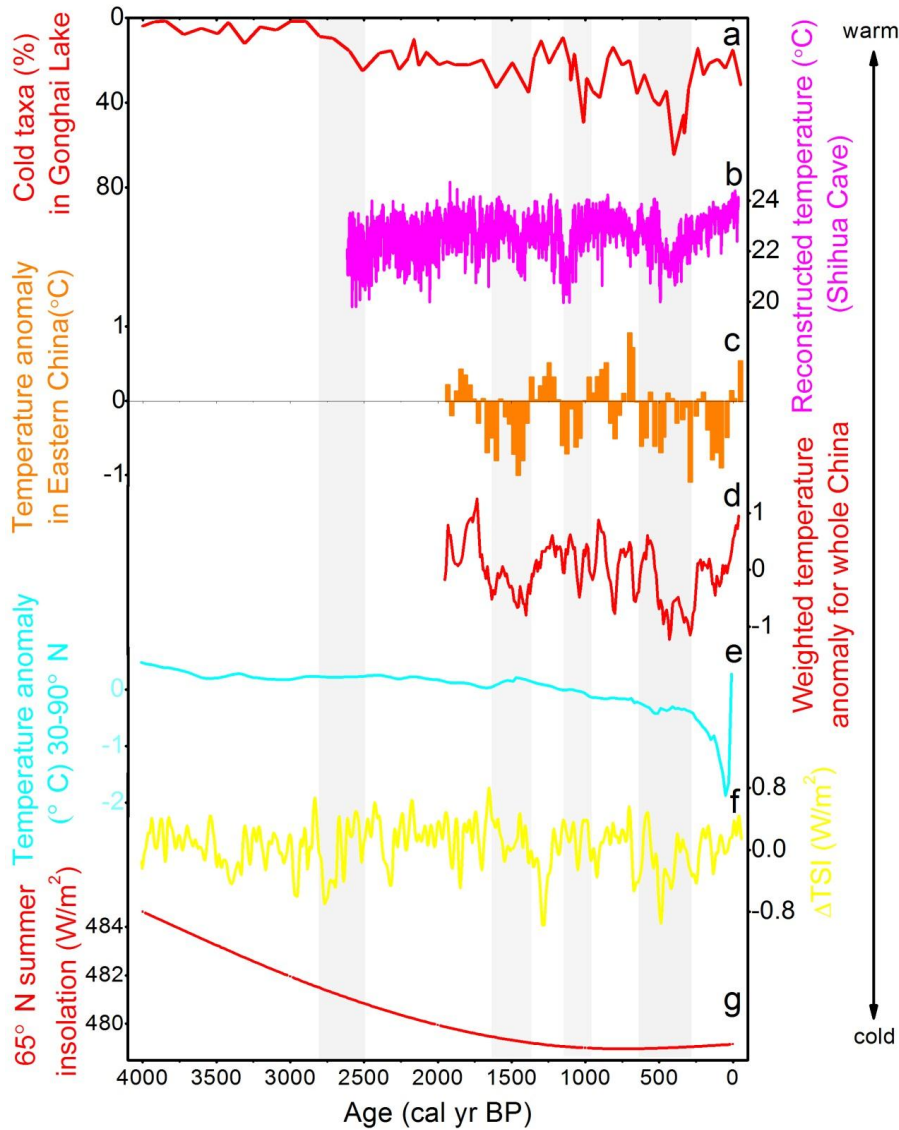
789

790 **Fig. 3**

792 **Fig. 4**



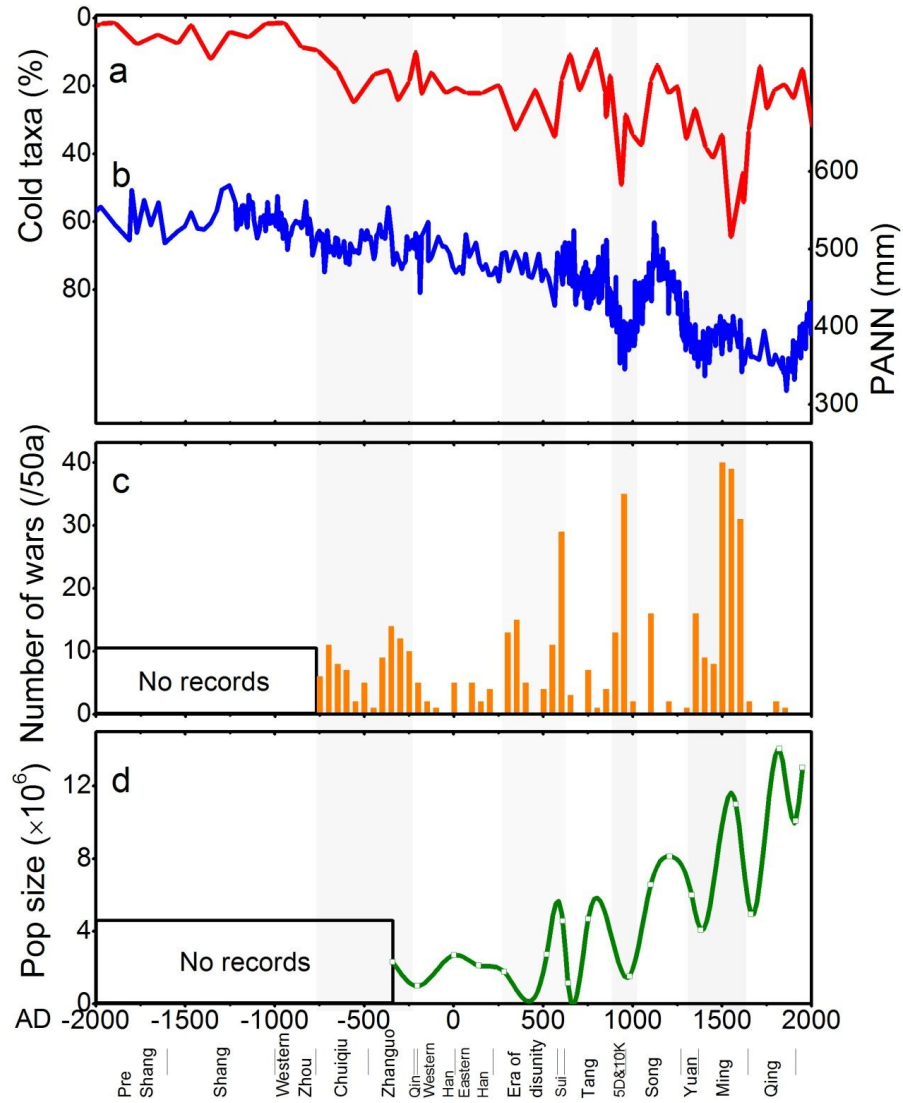
794 Fig. 5



795



796 Fig. 6



797